### **ORIGINAL PAPER**



# Analytical Models for the Chain-Length- and Velocity-Dependent Tribochemical Reaction Rates of Molecular Monolayers on Copper

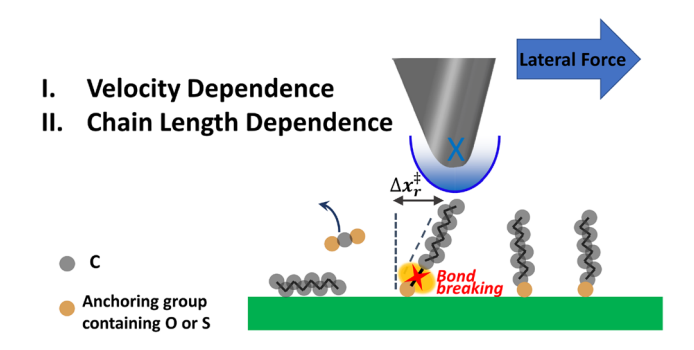
Octavio J. Furlong<sup>1</sup> · Sergio J. Manzi<sup>1</sup> · Kaiming Hou<sup>2</sup> · Resham Rana<sup>3</sup> · Heather Adams<sup>3</sup> · Wilfred T. Tysoe<sup>3</sup>

Received: 8 May 2023 / Accepted: 2 July 2023 © The Author(s), under exclusive licence to Springer Science+Business Media, LLC, part of Springer Nature 2023

#### Abstract

Previous work proposed a model potential for the interaction between a contact and the outermost surface of an organic overlayer that could be integrated into a Prandtl–Tomlinson model to analyze the velocity and temperature dependences of the friction force. The potential consisted of a parabola that extended to some cut-off distance when the energy reached a value of  $E^0_{sld}$ , which represents an activation barrier for the detachment of the tip from the molecular terminus. In addition to its simplicity, an advantage was that the potential also lent itself to being coupled to other degrees of freedom of the system. This feature was implemented by analyzing the friction of an interacting system between the tip-surface contact and a compliant molecular chain to yield velocity, temperature and chain-length dependences of the friction force that agreed well with experimental measurements of self-assembled monolayers (SAMs). This approach is extended here to allow the potential between the SAM and the surface to result in a chemical reaction by cleaving the bond between the hydrocarbon chain and the anchoring group, thus further emphasizing the versatility of this approach. The theory predicts that the tribochemical reaction rate should decrease with increasing chain length, in agreement with experimental results. Similar trends are seen for alkyl species that are used to cap lubricant additives such as in zinc dialkyl dithiophosphate (ZDDP). Measurements of the velocity dependence of the reaction of methyl thiolate species on copper showed little variation in accord with a lack of velocity dependence of the friction force.

## **Graphical Abstract**



Keywords Friction · Tribochemical reaction rates · Prandtl-Tomlinson model · Molecular monolayers

## 1 Introduction

Published online: 16 July 2023

Adsorbed long-chain hydrocarbons such as fatty acids often act as friction modifiers by forming an adsorbed overlayer on the surface to decrease the interaction between the outer surface of the film and the counterface

Extended author information available on the last page of the article

[1–4]. In these systems, the friction force is found to depend on the nature of the terminus of the hydrocarbon group, its surface orientation [5–7], and on the length of the hydrocarbon chain [1, 3, 4]. It has been conventionally proposed that this chain-length dependence is caused by an increase in the stiffness of the film due to the presence of intermolecular interactions. On the other hand, we



have analyzed the sliding friction of organic monolayers through a theoretical model that enabled the friction force to be described as a function of the hydrocarbon chain length that provided good agreement with experiment, without having to invoke intermolecular interactions [8]. This was accomplished by using a simplified, truncated parabola to mimic the tip-surface interaction potential, which was thus expected to be amenable to the development of analytical models. The validity of the analytical models was then confirmed by Monte Carlo simulations [9, 10]. A proposed advantage of this approach was that the potential could be easily coupled to other degrees of freedom of the system to enable more complex systems to be studied. This feature was exploited to calculate the friction of adsorbed, long-chain hydrocarbons in which the sliding potential between the tip and surface was coupled to a potential due to molecular tilting [8].

However, tribochemical reactions within the adsorbed layer can take place at higher stresses, and sometimes form low-friction carbonaceous films [1, 3, 7, 11, 12], thereby acting as chemically reactive lubricant additives. In addition, many additives are functionalized by hydrocarbon groups to enable them to dissolve in the base oil, and since their removal has been implicated in their reaction to form tribofilms [13–16], studies of the tribochemistry of carboxylic acids on surfaces may be relevant to understanding how other additives operate.

Lubricant additives often react by mechanochemical processes [17-24] in which the potential energy surface for the reaction is modified to change its rate [25–29]. Carbonaceous overlayers on surfaces react by the molecular chains tilting towards the surface [30, 31] to eventually induce bond scission. In the case of adsorbed alkyl thiolates on copper, this reaction cleaves a C-S bond to produce gas-phase hydrocarbons and sulfur [17, 21–24], but where shear also induces transport of sulfur into the subsurface region [28]. A similar tribochemical reaction occurs with carboxylates [32, 33], which form spontaneously on copper following exposure to carboxylic acids, except that the cleavage of the C-COO bond eliminates carbon dioxide. No other side reactions were found for this initial decomposition step. This molecular tilting motion is similar to that used for the analysis of SAM friction [9], so that it is relatively straightforward to modify the friction model to incorporate a reactive tilting potential to enable surface-chemical processes to be described.

The analysis presented below shows how the reaction rates of adsorbed carboxylates depend on the chain-length and how the tribochemical reaction of a methyl thiolate overlayer depends on the sliding velocity. We note that the actual situation can be more complicated than addressed by these simple analyses. For example, it has been found that the shear-induced reactions of short-chain thiolates

exhibit interesting phenomena in which some critical force is required to induce a reaction [34]. This effect is not included in the analysis below.

## 2 Analysis of Tribochemical Reaction Rates

On one hand, the analysis can be carried out using potentials coupled to a constant-force sliding potential such as found in a conventional tribometer. In this case, a constant normal load and force is applied to the system as a constraint, and the counterface is slid at a constant velocity to induce a mechanochemical reaction. Here, the rate can be measured from the evolution of the friction force [17] due to a change in composition of the rubbed region [21, 35], or from the evolution of gas-phase products formed by sliding [30]. On the other hand, a reaction can also be induced by compliant sliding as in an atomic-force microscope (AFM) tip sliding over the molecular layer adsorbed on the surface [32, 36, 37]. Since there are few results available for the mechanochemical decomposition of SAMs by a sliding AFM tip that could be used to test the resulting models, the analysis presented here is restricted to shear-induced reactions for constant-force sliding under a constant load. The effect of changing the normal force will be included later.

## 2.1 Mechanochemistry Under Constant-Force Sliding

Following previous analyses of the coupled sliding of self-assembled monolayers on solid surfaces, and as depicted in Fig. 1 [8, 9], the sliding surface potential due to the interaction of the tip with the surface is given by:

$$V_s(x) = \frac{1}{2}k_s x^2$$
 or  $V_s(x) = E_S^o \left(\frac{x}{\Delta x_s^{\ddagger}}\right)^2$ , (1)

where x represents the displacement from the minimum of a harmonic sliding potential with force constant  $k_s = 2E_S^o/\Delta x_s^{\ddagger 2}$ , where  $\Delta x_s^{\ddagger}$  is known as an activation length, in this case for sliding, and  $E_S^o$  is the height of the sliding potential when  $x = \Delta x_s^{\ddagger}$ . Since the tip can detach from the terminus of one adsorbate and subsequently attach to the next one, this is considered to be a reactive potential, in which the detachment (or sliding) energy barrier vanishes at a distance  $x = \Delta x_s^{\ddagger}$ , where  $V_s(\Delta x_s^{\ddagger}) = E_S^o$  [8].

On the other hand, the corresponding tilting potential of the self-assembled monolayer chain is given by:

$$V_t(\theta) = \frac{1}{2} k_\theta^t \theta^2 \text{ or } V_t(x_0) = \frac{1}{2} k_t x_0^2,$$
 (2)



Tribology Letters (2023) 71:86 Page 3 of 9 86

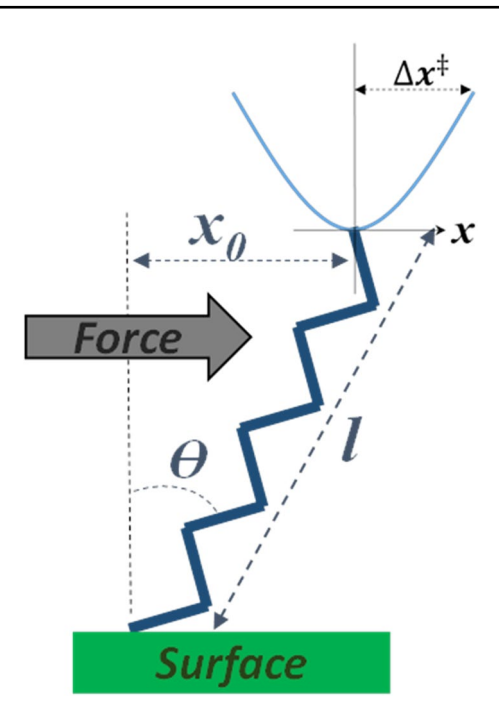


Fig. 1 Schematic depiction of the coupled adsorbate system used to analyze self-assembled monolayer friction and mechanochemistry

where, for relatively small angles, the tilt of the SAM chain from the normal is  $\theta \approx x_0/l$ , where l is the chain length, so that  $k_t = k_\theta^t/l^2$  (see Figure 1). By describing the system as two coupled harmonic springs, where the force balance gives  $k_s x = k_t x_0$ , we arrive to the following overall potential energy of the system under the influence of a constant lateral force  $F_L$ :

$$V_S(x, x_0, F_L) = \frac{1}{2}k_s x^2 - F_L(x + x_0)$$

or

$$V_S(x, F_L) = \frac{1}{2}k_s x^2 - F_L \alpha_s x,\tag{3}$$

where  $\alpha_s = \left(1 + \frac{k_s}{k_t}\right)$ . Note that the potential energy could be similarly written as  $V_S(x_0, F_L)$ , but leads to the same final results as for Eqn. (2). This potential shows how the energy provided by the external force,  $F_L(x+x_0)$ , is stored in the system to decrease the energy barrier required to slide (detach) from one adsorbate to attach to the next. The new adsorbate configuration induced by the force is found by minimizing the potential energy to give  $x(F_L) = \frac{\alpha_s}{k_s} F_L$ . From the relationship between x and  $x_0$  given above, we can also write  $x_0(F_L) = \frac{\alpha_s}{k_s} F_L$ . By calculating the force-dependent initial- and transition-state energies, we can arrive at a sliding energy barrier given by:

$$E_{act}^{S}(F_{L}) = \frac{\alpha_{s}^{2}}{2k_{s}}(F_{s}^{*} - F_{L})^{2},$$
(4)

where  $F_s^* = \frac{k_s \Delta x_s^3}{a_s}$ , which corresponds to a critical force at which the energy barrier due to sliding decreases to zero. Note that Eq. 4 can be simplified to give  $E_{act}^S(F_L) = E_s^0 \left(1 - \frac{F_L}{F_s^*}\right)^2$ , confirming that  $E_{act}^S(F_L) \to E_s^0$  as  $F_L \to 0$ , as it should.

## 2.2 Modeling Chemical Reaction Rates

We now also consider the possibility of a chemical reaction being induced by the adsorbed molecule tilting. As indicated above, this motion initiates the reaction on the surface until a point is reached at which the orbitals in the adsorbed molecule can interact with those in the surface and weaken the bond between the hydrocarbon chain and the surface anchoring group to ultimately induce bond scission. In the case of an anchored alkyl chain, the bond cleavage products can undergo a facile β-hydride elimination reaction to form a 1-alkene [38–40]. If the chain terminus contains an unsaturated terminal group such that it can interact with the substrate, this limits the probability of it undergoing a hydride-elimination reaction, thereby allowing the hydrocarbon fragment to polymerize on the surface instead [36]. It is likely that analogous reactions occur for alkyl chains that are incorporated in lubricant additives to facilitate their solubility in the base lubricating oil [20].

This surface chemical reaction can be described by a parabolic reaction potential that also leads to bond cleavage (detachment) and the formation of reaction product(s), with some activation barrier  $E^R_{act}$  [9]. Note that the present model differs from that used to describe the chain-length dependence of sliding friction, where the tilting potential was not allowed to undergo a chemical reaction [8]. This further illustrates the flexibility of this approach, which enables the effects of coupling between interacting processes to be modeled, where these processes can be designated as reactive or unreactive (i.e., only dissipative) ones. Thus, the potential due to a reaction induced by tilting can be written as:

$$V_r(\theta) = \frac{1}{2} k_\theta^r \theta^2 \quad \text{or} \quad V_r(x_0) = \frac{1}{2} k_r x_0^2,$$
 (5)

where again  $\theta \approx x_0/l$ , so that  $k_r = k_\theta^r/l^2$ . It is expected that the value of  $k_\theta^r$  depends only on the nature of the anchoring group and is thus likely to be relatively independent of the length of the carbonaceous chain. Similar to the analysis for the sliding potential, the energy barrier for reaction vanishes at a critical angle  $\Delta \theta^{\ddagger}$ , which occurs at a lateral displacement of the molecular terminus  $\Delta x_r^{\ddagger} = \Delta \theta^{\ddagger} l$ . It is assumed that the barrier for SAM decomposition occurs at similar values of  $\Delta \theta^{\ddagger}$  irrespective of the chain length. This is a reactive



potential so that, analogous to the sliding potential, the energy barrier for the reaction is given by  $E^R_{act}$ . In this case, the potential in Eq. 2 can also be written as  $V_r(x_0) = E^o_R \left(\frac{x_0}{\Delta x_r^{\frac{1}{2}}}\right)^2$ , so that  $k_r = 2E^o_R/\Delta x_r^{\frac{1}{2}^2}$ .

Given that the maximum of the reaction potential is located at  $x_0 = \Delta x_r^{\ddagger}$ , then  $E_R^{max} = E_R^o$ , while the minimum of the potential moves to  $x_0(F_L)$  under the influence of an applied lateral force  $F_L$  to give:  $E_R^{min} = E_R^o \left(\frac{\alpha_s}{k_t \Delta x_r^2}\right)^2 F_L^2$ . This yields an equation for the force-dependent reaction energy barrier for SAM decomposition as:

$$E_{act}^{R}(F_L) = E_R^o \left( 1 - \left( \frac{\alpha_s}{k_t \Delta x_r^{\ddagger}} \right)^2 F_L^2 \right). \tag{6}$$

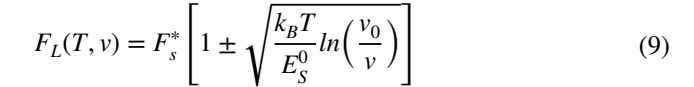
In order to obtain the overall velocity and temperature dependences of the mechanochemical reaction rates, and since both processes (sliding and reaction) lead to detachment, either between the tip and the molecular terminus (sliding), or from the molecule and the surface (reaction), we can conclude that:

$$k^s + k^r = \frac{v}{\Delta x_s^{\ddagger}},\tag{7}$$

where  $k^s$  and  $k^r$  are the rate constants for the transitions due to sliding and reaction, respectively, v is the sliding velocity, and  $\Delta x_s^{\ddagger}$  is the distance from the reactant to the transition state that controls the transit time from one site to the next [41, 42]. This analysis assumes that the energy required to transit the barrier is rapidly dissipated after the transition occurs. Furthermore, since they are thermally activated processes:

$$\begin{split} k^{s} &= A_{s} exp \Biggl( -\frac{E_{act}^{S} \bigl( F_{L} \bigr)}{k_{B}T} \Biggr) \quad \text{and} \\ k^{r} &= A_{r} exp \Biggl( -\frac{E_{act}^{R} \bigl( F_{L} \bigr)}{k_{B}T} \Biggr), \end{split} \tag{8}$$

where  $A_s$  and  $A_r$  are pre-exponential factors for sliding and for the surface reaction, respectively. However, in general, the rate of the tip sliding over the surface  $k^s$  is much larger than the reaction rate constant,  $k^r$ , given that it generally takes multiple passes of a tip over the surface for the reaction to be completed. If the reaction rate constant were much faster than the sliding rate constant, the reverse would be true and the overlayer would be depleted very rapidly, which is usually not the case. Therefore, it can be assumed that  $A_s exp\left(-\frac{E_{act}^S(F_L)}{k_BT}\right) \cong \frac{v}{\Delta x_s^2}$ , or  $E_{act}^S(F_L) = k_BTln\left(\frac{v_0}{v}\right)$ , where  $v_0 = A_s\Delta x_s^2$ . Substituting for  $E_{act}^S(F_L)$  from Eq. 4 gives an equation for the velocity- and temperature-dependences of the sliding friction force as:



As can be observed in Eq. 6, the term in brackets does not depend on the SAM chain length, which is included in  $F_s^*$ . Therefore, in order to evaluate the effect of chain length on friction, it is convenient to write:  $F_L(T, v) = F_s^*[1 - B(T, v)]$ , where  $B(T, v) = \sqrt{\frac{k_B T}{E_s^0} ln\left(\frac{v_0}{v}\right)}$ . Furthermore,  $F_s^*(l) = \frac{k_s \Delta x_s^2}{\left(1 + \frac{k_s L}{k_s^2}\right)}$ , and

has been shown to yield results that are in good agreement with the experimentally measured chain-length dependence of the friction force of carboxylate SAMs on copper [8]. We can now substitute the lateral force into Eq. 6 to obtain an equation for  $E_{act}^R(T, v.l)$  as:

$$E_{act}^{R}(T, v, l) = E_{R}^{o} \left( 1 - \left( \frac{\alpha_{s}}{k_{t} \Delta x_{r}^{\ddagger}} \right)^{2} F_{s}^{*2} [1 - B(T, v)]^{2} \right). \tag{10}$$

Finally, substituting for  $F_s^*$  leads to:

$$E_{act}^{R}(T, \nu, l) = E_{R}^{o} \left( 1 - \left( \frac{k_{s} \Delta x_{s}^{\ddagger}}{k_{\theta}^{t} \Delta \theta^{\ddagger}} \right)^{2} l^{2} [1 - B(T, \nu)]^{2} \right). \tag{11}$$

Therefore, assuming that  $\Delta\theta^{\ddagger}$  and  $k_{\theta}^{t}$  are identical for all molecular chain lengths yields a formula for the temperature, velocity and chain-length dependences of the decomposition activation energy for SAMs on surfaces. The validity of Eq. 8 is tested experimentally for the velocity-dependence of the mechanochemical reaction rate of methyl thiolate species on copper [17, 21–24] and for the chain length dependence of the reaction of carboxylates on copper [32, 34, 36].

## 3 Experimental and Theoretical Methods

Experiments were carried out in UHV chambers operating at pressures of  $\sim 2.0 \times 10^{-10}$  Torr after bakeout. Ball-onflat friction measurements were made in a UHV chamber, which has been described in detail elsewhere [43]. The chamber was equipped with a UHV-compatible tribometer, which simultaneously measures normal loads, lateral forces and the electrical contact resistance between the tip and substrate. Previous work has shown that the maximum interfacial temperature rise for a copper sample under these conditions is much less than 1 K [35]. The spherical pin ( $\sim 1.27 \times 10^{-2}$  m diameter) was made from tungsten carbide containing some cobalt binder, and could be cleaned by electron bombardment heating in vacuo or by argon ion bombardment; for the experiments reported here, it was cleaned by heating. The pin was attached to an arm that has two strain gauges that



Tribology Letters (2023) 71:86 Page 5 of 9 86

enable the measurement of the lateral force as well as the normal load applied on the surface. The normal load is set and controlled by the LabView control software to a preset value. The arm was mounted to a rotatable Conflat flange to allow the pin to be rotated to face a cylindrical-mirror analyzer (CMA) to enable Auger analyses of both the pin surface and the copper sample [28].

The copper foil sample was prepared by mechanical polishing using sandpapers of decreasing grit size until no visible scratches were observed. This was followed by polishing using polycrystalline diamond paste until a visibly smooth surface was seen under a microscope. The sample was mounted to a UHV-compatible, precision x, y, z manipulator for measuring the elemental profiles across a rubbed region of the sample under UHV conditions. The copper foil sample was cleaned using a standard procedure consisting of cycles of Ar<sup>+</sup> bombardment with subsequent annealing to 850 K for 10 min. Ar<sup>+</sup> bombardment was performed at a background gas pressure of  $\sim 5.0 \times 10^{-5}$  Torr at a 1 kV potential, while maintaining a  $\sim 2~\mu A$  sample current.

The mechanochemical reaction rates were measured from the variation in the friction coefficient as a function of the number of rubbing cycles [17]. Assuming that the reaction occurs via first-order reaction kinetics, then the reactant coverage  $\theta_R$  is given by  $\theta_R(t) = \theta_R^0 \exp(-k_r t)$ . However, if the time that the tip takes to pass over the surface is given by  $t_p$  and the number of passes is p, then  $\theta_R(p) = \theta_R^0 \exp(-k_r^p p)$ , where  $k_r^p = k_r t_P$ . The product coverage is then given by  $\theta_P = 1 - \theta_R = 1 - \theta_R^0 \exp(-k_r^p p)$ . If the reactant and the product have different friction coefficients,  $\mu_R$  and  $\mu_P$ , then the resulting friction coefficient will be  $\mu(p) = \mu_R \exp(-k_r^p p) + \mu_P (1 - \exp(-k_r^p p))$  or  $\mu(p) = \mu_P + (\mu_R - \mu_P) \exp(-k_r^p p)$ , which allows the reaction rate to be measured. The values of  $\mu_R$  and  $\mu_P$  are obtained by fitting to the experimental data, where  $\mu_R$  varies from ~0.34 to ~0.27 depending on the chain length as described previously [8], and  $\mu_P$  is the final value close to that found for clean copper [35]. The DMDS (Aldrich, 99.0% purity), propionic acid (Sigma Aldrich, ≥ 90 purity), butanoic acid (Sigma Aldrich, ≥99.0 purity), pentanoic acid (Sigma Aldrich, ≥ 98.0 purity), hexanoic acid (Sigma Aldrich, ≥ 99% purity), heptanoic acid (Sigma Aldrich, ≥ 99.0% purity) and octanoic acid (Sigma Aldrich, ≥98.0% purity) were transferred to glass bottles and attached to the gas-handling system of the vacuum chamber, where they were subjected to several freeze-pump-thaw cycles. Their purity was monitored using mass spectroscopy.

## 4 Results and Discussion

The sliding-induced reaction rates were measured from the evolution in the friction force as a function of the number of passes over the surface, where the friction evolves from that of the reactant to that of the product, and the intermediate friction is taken to scale with the relative coverages of the surface species. This enables in-situ tracking of the way the adsorbate coverages change as a function of time, allowing a surface reaction rate constant to be measured [17]. This approach will be used to test the validity of Eq. 8, which describes the chain-length- and velocity-dependences of shear-induced decomposition of adsorbed overlayers. The temperature-dependence was not measured because of the difficulty in correctly monitoring the temperature at a sliding solid–solid interface.

## 4.1 Chain-Length Dependence of Tribochemical Reaction Rates

The chain-length dependences of the rates of shear-induced decomposition of carboxylates on copper were measured using a series of carboxylic acids adsorbed on a clean copper substrate in UHV to create the corresponding carboxylate overlayers [32, 33, 36, 44–46] using a background pressure of  $\sim 10^{-7}$  Torr, which is much lower than the vapor pressure of the compounds. The structure and surface chemistry of carboxylates on copper have been studied using Auger and reflection-absorption infrared (RAIRS) spectroscopies in a previous work [8]. Specifically, in the Auger analyses, the peak-to-peak intensity ratios of carbon and oxygen KLL signals to the copper KLL signal are consistent with the carboxylate forming overlayers on copper with similar saturation coverages. The infrared spectroscopy results reveal that the carboxylates bind to a copper surface in a bidentate configuration and the hydrocarbon chains extend upward to form a uniform overlayer. In RAIRS spectra, infrared peak shifts can be characteristic of the order and packing density. For example, heating the sample from 92 to 203 K causes the asymmetric methylene stretching peak to shift from 2020 to 2016 cm<sup>-1</sup> and the C-H bending mode frequency to change from 1470 to 1463 cm<sup>-1</sup>, suggesting an increase in structural order.

The results are shown in Fig. 2 for measurements at a constant sliding speed, load and temperature. The data were fit to the exponential growth formulae derived in the Experimental and Theoretical Methods section to obtain values of the rate constants per pass,  $k_p$ . The fits to the results are also shown as red lines in Fig. 2, and the resulting plot of the rate constants as a function of the number of carbon atoms in the alkyl chain is shown in Fig. 3.



86 Page 6 of 9 Tribology Letters (2023) 71:86

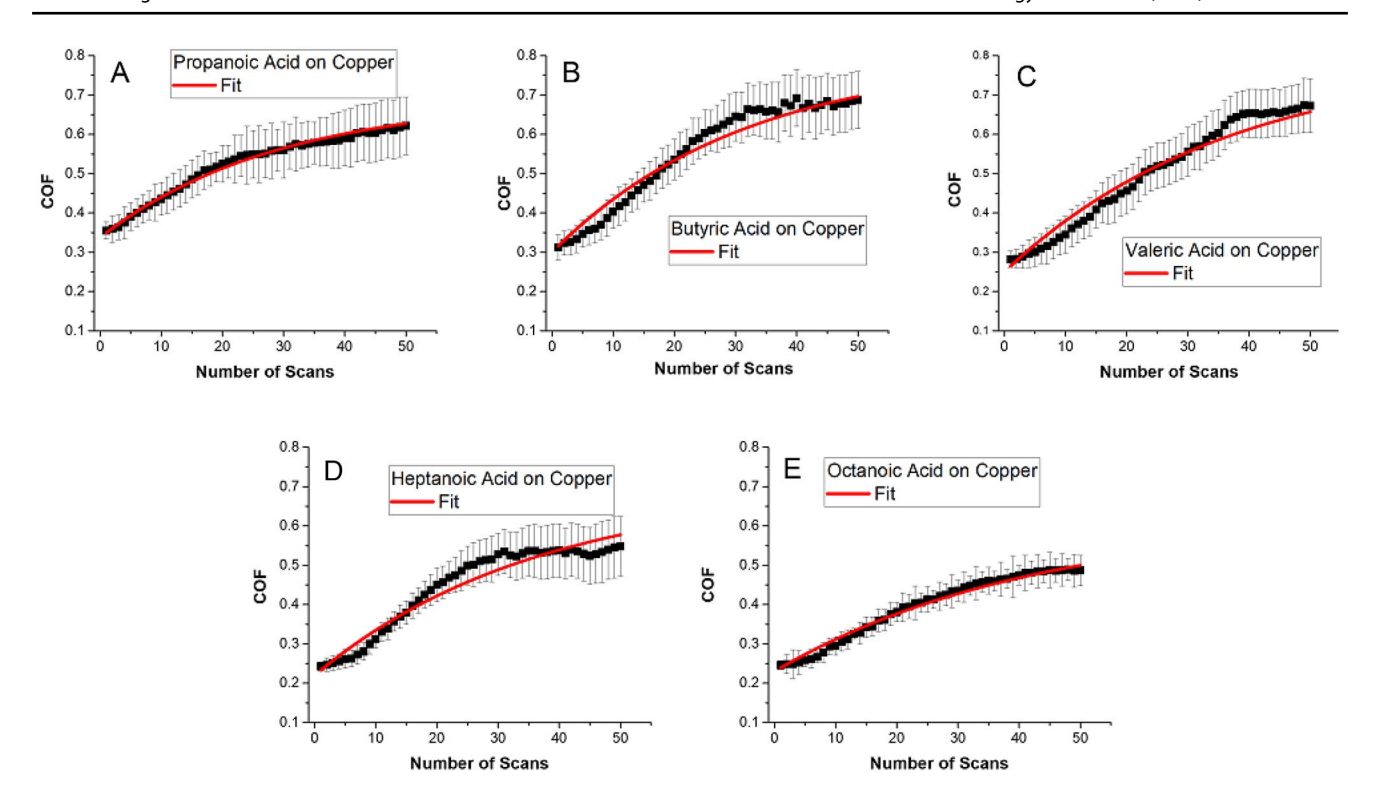
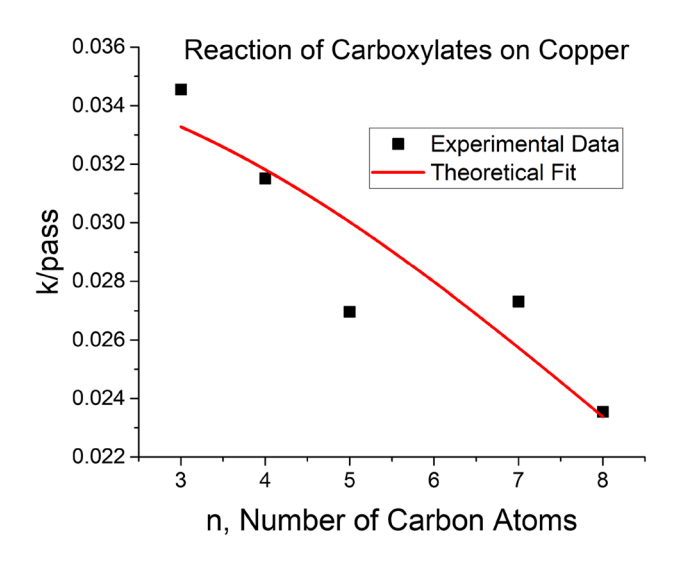


Fig. 2 Plot of friction coefficient versus number of scans measured in the UHV tribometer for carboxylate overlayers on copper, measured at a sliding speed of 4 mm/s with a normal load of 0.44 N for A propanoic, B butyric, C valeric, D heptanoic and E octanoic acid



**Fig. 3** Plots of the tribochemical reaction rate of a series of carboxylate adsorbed on a clean copper substrates measure un UHV as a function of the number of carbon atoms in the carboxylic acid

The energy barrier varies as a function of chain length as g i v e n b y E q . 8 , which gives  $E^R_{act}(l) = E^o_R \left(1 - \left(\frac{k_s \Delta x_s^2}{k_o^2 \Delta \theta^2}\right)^2 l^2 [1 - B(T, v)]^2\right) = E^o_R - K(T, v) l^2 \qquad \text{where } e$   $K(T, v) = E^o_R \left(\frac{k_s \Delta x_s^2}{k_o^2 \Delta \theta^2}\right)^2 [1 - B(T, v)]^2. \text{ The reaction rate constant } k^r(l)$  is then given by  $k^r(l) = A_R exp\left(-E^R_{act}(l)/k_BT\right)$ . Substituting

gives  $k^r(l) = k_0^r exp(K(T, v)l^2/k_BT)$ , where  $k_0^r$  is the rate constant for reaction at  $F_L = 0$ . It has been previously shown that the length of the chain can be written as  $l \sim d_{coo} + d_{cc}(n-1)$ , where  $d_{coo}$  is the contribution from the carboxylate anchoring group,  $d_{cc}$  is the projection of the carbon–carbon bond length along the chain, and n is the number of carbon atoms in the alkyl chain [8]. If  $d_{coo}\cong d_{cc},$  then the length of the *n*-carbon chain is  $l \sim d_{CC}n$ . This gives an equation for the overall chain-length dependence of the reaction rate constant as a function of the number of carbon atoms in the chain as  $k_R(n)=k_0^r exp\left(P(T,v)n^2\right)$ , where  $P(T,v)=K(T,v)/d_{CC}^2k_BT$ . This equation is plotted in red on the data in Fig. 3, and leads to good agreement with the experimental data, with  $k_R(n) = 0.035 \pm 0.002$  per pass, and  $P(T, v) = -6.4 \pm 1.3 \times 10^{-3}$  at a sliding speed of 4 mm/s and a temperature of 293 K. This suggests that longer chains are less reactive than shorter ones. Note that these results do not include shorter-chain carboxylates on copper because they show anomalous critical behavior [34]. Similar trends have been found for the reactivity of functional groups on zinc dialkyl dithiophosphate (ZDDP), in which oct-1-yl functionalized ZDDP reacts more rapidly than ZDDP functionalized by dodec-1-yl groups [20], suggesting that similar chainlength trends occur with functionalized lubricant additives as for self-assembled monolayer friction modifiers. Similar



Tribology Letters (2023) 71:86 Page 7 of 9 86

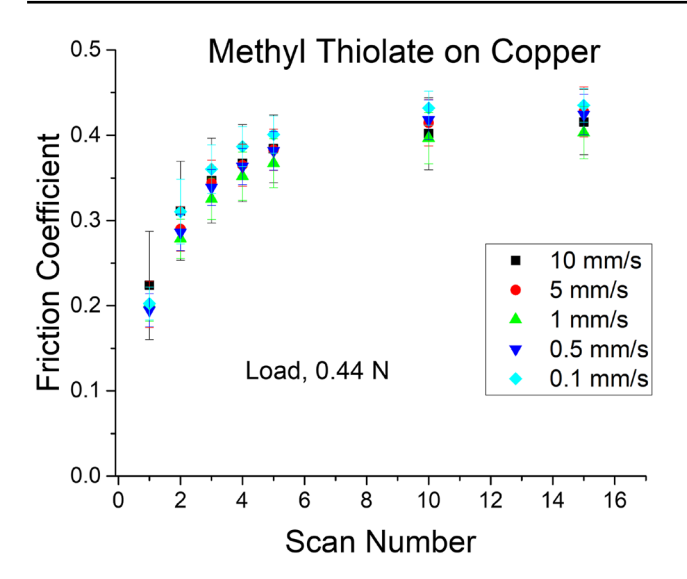


**Fig. 4** Plot of the evolution in friction for a saturated methyl thiolate overlayer on a clean copper substrate measured in UHV at a temperature of 298 K and a normal load of 0.44 N

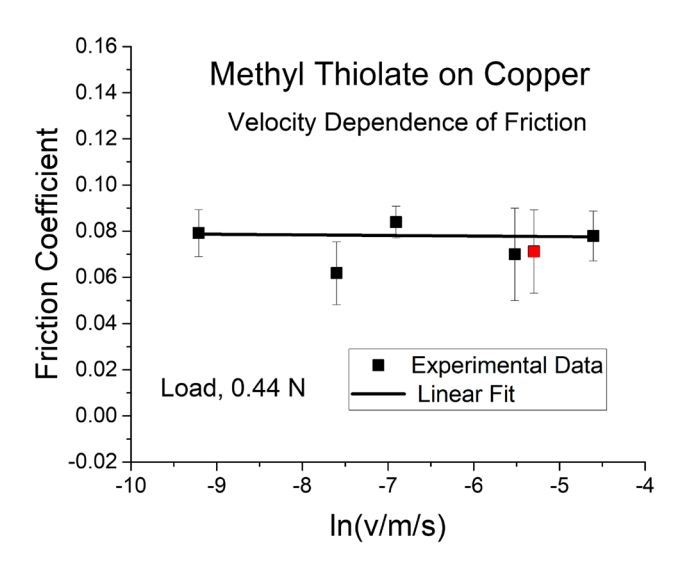


**Fig. 5** Plot of the friction coefficient versus ln(sliding speed) for a saturated methyl thiolate overlayer on a clean copper substrate (filled black square) measured in UHV at a temperature of 298 K and a normal load of 0.44 N. Shown for comparison is the result obtained using a sliding speed of 4 mm/s (filled red square) [17]

effects have also been seen for the reactivity of ionic liquids [47].

## 4.2 Velocity Dependence of Tribochemical Reaction Rates

The reaction rates of methyl thiolate species adsorbed on a copper substrate were measured as a function of sliding speed over two orders of magnitude, from 0.1 to 10 mm/s.

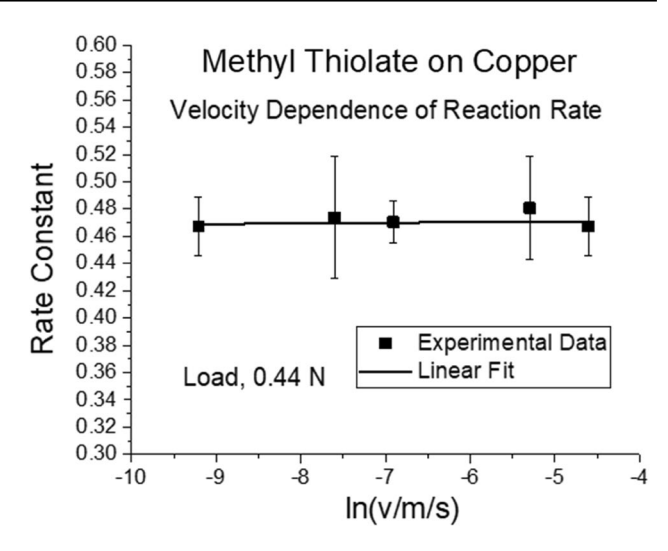


**Fig. 6** Plot of the reaction rate constant versus ln(sliding speed) for the reaction of a saturated methyl thiolate overlayer on a clean copper substrate (filled black square) measured in UHV at a temperature of 298 K and a normal load of 0.44 N

As above, the variation in friction coefficient as a function of the number of scans is taken to represent the surface reaction kinetics and is used to test the above theoretical analysis. The fits to that data on Fig. 4 yield both the initial friction coefficient and the reaction rate as a function of the sliding velocity. In order to gain insights into the value of the parameter B(T, v) that controls the friction (Eq. 6), the friction force is shown plotted in Fig. 5 as a function of the sliding velocity. The reproducibility of the data is demonstrated by comparing with previous results from a different sample ( ) [17], which agrees well with the current data. This shows that the friction coefficient at a constant normal load of 0.44 N is ~0.08. This lack of variation with velocity indicates that  $B(T, v) \ll 1$  so that  $F_I(T, v) \sim F_c^*$ . In this case, from Eq. 8, the reaction activat i o n e n e r g y b e c o m e s  $E_{act}^R(T,v,l) = E_R^o \left( 1 - \left( \frac{k_x \Delta x_x^2}{k_x^2 \Delta \theta^2} \right)^2 l^2 \right) = E_R^o - K(T,v) l^2. \text{ Now, as above,}$  $k_R(v) = k_0^r exp(P(T, v)n^2)$ , where  $P(T, v) = K(T, v)/d_{CC}^2 k_B T$ . Since the reaction rate is constant and n = 2 for a methyl thiolate overlayer,  $k_R(v) = k_0^r exp(4P(T, v))$ , and is independent of the sliding velocity as shown in Fig. 6. However, since (P(T, v)) is small, the exponential will be close to unity, suggesting that  $k_0^r \sim 0.48$ . Thus, while variations in friction force with velocity have been measured using nanoscale contacts in an AFM [48–50], the larger sliding speeds and the contact conditions in macroscale contacts suggest that the parameter B(T, v) in Eq. 6 is less than unity and results in mechanochemical reaction rates that are independent of the sliding speed as also observed by others [51].



86 Page 8 of 9 Tribology Letters (2023) 71:86

## 5 Conclusions

A coupled model has been developed using a reactive interaction potential that consists of a truncated parabola to describe the tribochemical reaction rates of adsorbed SAMs as a function of chain length and sliding speed. Similar models have been used to calculated the chain-length dependence of sliding friction [8] by implementing the potential in a Prandtl-Tomlinson friction model both for constantforce and compliant sliding as measured in an atomic-force microscope. Both models yielded good agreement with experimental results. This work illustrated how the model can be extended to systems with coupled potentials. The analysis in this paper extends these ideas to a coupled system in which the SAM-substrate potential is rendered reactive by using a truncated parabola in which the potential energy becomes constant at some critical distance with an energy that corresponds to the activation energy for the reaction. This model is analyzed only for constant-force sliding, for which there are available results with which to compare, to calculate velocity, temperature and chain-length dependence of tribochemical reaction rates. The theoretical results provide good agreement with experimental measurements for the chain-length dependence of the reactivity of carboxylate SAMs on copper and with the velocity dependence of the reaction rate of methyl thiolate overlayers on copper.

Acknowledgements We gratefully acknowledge the Civil, Mechanical and Manufacturing Innovation (CMMI) Division of the National Science Foundation under grant number 2020525 for support of this work. KH acknowledges support from the China Scholarship Council.

**Author Contributions** All authors contributed equally to this work.

**Funding** Funding was provided by National Science Foundation (Grant No. CMMI-2020525), and a Distinguished International Students Scholarship from the China Scholarship Council.

Data Availability Original results are available on reasonable request.

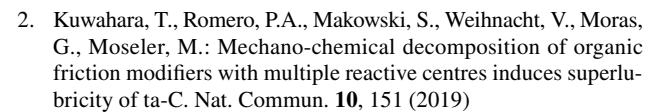
## **Declarations**

Conflict of interest The authors declare that they have no conflicts of interest.

**Ethical Approval** All ethical responsibilities were respected by the authors.

## References

 De Barros Bouchet, M.I., Martin, J.M., Forest, C., le Mogne, T., Mazarin, M., Avila, J., et al.: Tribochemistry of unsaturated fatty acids as friction modifiers in (bio)diesel fuel. RSC Adv. 7, 33120–33131 (2017)



- Campen, S., Green, J.H., Lamb, G.D., Spikes, H.A.: In situ study of model organic friction modifiers using liquid cell AFM; saturated and mono-unsaturated carboxylic acids. Tribol. Lett. 57, 18 (2015)
- 4. Spikes, H.: Friction modifier additives. Tribol. Lett. 60, 5 (2015)
- Brewer, N.J., Beake, B.D., Leggett, G.J.: Friction force microscopy of self-assembled monolayers: influence of adsorbate alkyl chain length, terminal group chemistry, and scan velocity. Langmuir 17, 1970–1974 (2001)
- Mikulski, P.T., Herman, L.A., Harrison, J.A.: Odd and even model self-assembled monolayers: links between friction and structure. Langmuir 21, 12197–12206 (2005)
- Lundgren, S.M., Ruths, M., Danerlöv, K., Persson, K.: Effects of unsaturation on film structure and friction of fatty acids in a model base oil. J. Colloid Interface Sci. 326, 530–536 (2008)
- 8. Hou, K., Bavisotto, R., Manzi, S.J., Perez, E.J., Furlong, O.J., Kotvis, P., et al.: Prandtl–Tomlinson-type models for coupled molecular sliding friction: chain-length dependence of friction of self-assembled monolayers. Tribol. Lett. 70, 66 (2022)
- Manzi, S.J., Carrera, S.E., Furlong, O.J., Kenmoe, G.D., Tysoe, W.T.: Prandtl–Tomlinson-Type models for molecular sliding friction. Tribol. Lett. 69, 147 (2021)
- Binder, K.: Monte Carlo Methods in Statistical Physics. Springer, Berlin (1986)
- De Barros Bouchet, M.I., Martin, J.M., Avila, J., Kano, M., Yoshida, K., Tsuruda, T., et al.: Diamond-like carbon coating under oleic acid lubrication: Evidence for graphene oxide formation in superlow friction. Sci. Rep. 7, 46394 (2017)
- Kano, M., Martin, J.M., Yoshida, K., De BarrosBouchet, M.I.: Super-low friction of ta-C coating in presence of oleic acid. Friction 2, 156–163 (2014)
- Dickert, J.J., Rowe, C.N.: Thermal decomposition of metal O, O-dialkyl phosphorodithioates. J. Org. Chem. 32, 647–653 (1967)
- Jones, R.B., Coy, R.C.: The chemistry of the thermal degradation of zinc dialkyldithiophosphate additives. ASLE Trans. 24, 91–97 (1981)
- Mosey, N.J., Woo, T.K.: A quantum chemical study of the unimolecular decomposition mechanisms of zinc dialkyldithiophosphate antiwear additives. J. Phys. Chem. A 108, 6001–6016 (2004)
- Mosey, N.J., Müser, M.H., Woo, T.K.: Molecular mechanisms for the functionality of lubricant additives. Science 307, 1612–1615 (2005)
- Adams, H., Miller, B.P., Kotvis, P.V., Furlong, O.J., Martini, A., Tysoe, W.T.: In situ measurements of boundary film formation pathways and kinetics: dimethyl and diethyl disulfide on copper. Tribol. Lett. 62, 1–9 (2016)
- Gosvami, N.N., Bares, J.A., Mangolini, F., Konicek, A.R., Yablon, D.G., Carpick, R.W.: Mechanisms of antiwear tribofilm growth revealed in situ by single-asperity sliding contacts. Science 348, 102–106 (2015)
- Zhang, J., Spikes, H.: On the mechanism of ZDDP antiwear film formation. Tribol. Lett. 63, 1–15 (2016)
- Zhang, J., Ewen, J.P., Ueda, M., Wong, J.S.S., Spikes, H.A.: Mechanochemistry of zinc dialkyldithiophosphate on steel surfaces under elastohydrodynamic lubrication conditions. ACS Appl. Mater. Interfaces 12, 6662–6676 (2020)
- Furlong, O.J., Miller, B.P., Kotvis, P., Tysoe, W.T.: Low-temperature, shear-induced tribofilm formation from dimethyl disulfide on copper. ACS Appl. Mater. Interfaces 3, 795–800 (2011)
- Furlong, O., Miller, B., Tysoe, W.T.: Shear-induced boundary film formation from dialkyl sulfides on copper. Wear 274–275, 183–187 (2012)



Tribology Letters (2023) 71:86 Page 9 of 9 86

- Miller, B., Furlong, O., Tysoe, W.: The kinetics of shear-induced boundary film formation from dimethyl disulfide on copper. Tribol. Lett. 49, 39–46 (2013)
- Adams, H., Miller, B.P., Furlong, O.J., Fantauzzi, M., Navarra, G., Rossi, A., et al.: Modeling mechanochemical reaction mechanisms. ACS Appl. Mater. Interfaces. 9, 26531–26538 (2017)
- Spikes, H., Tysoe, W.: On the commonality between theoretical models for fluid and solid friction, wear and tribochemistry. Tribol. Lett. 59, 1–14 (2015)
- Tysoe, W.: On stress-induced tribochemical reaction rates. Tribol. Lett. 65, 48 (2017)
- Boscoboinik, A., Olson, D., Adams, H., Hopper, N., Tysoe, W.T.: Measuring and modelling mechanochemical reaction kinetics. Chem. Commun. 56, 7730–7733 (2020)
- Rana, R., Long, D., Kotula, P., Xu, Y., Olson, D., Galipaud, J., et al.: Insights into the mechanism of the mechanochemical formation of metastable phases. ACS Appl. Mater. Interfaces 13, 6785–6794 (2021)
- James, J., Saldin, D.K., Zheng, T., Tysoe, W.T., Sholl, D.S.: Structure and binding site of acetate on Pd(111) determined using density functional theory and low energy electron diffraction. Catal. Today 105, 74–77 (2005)
- Adams, H.L., Garvey, M.T., Ramasamy, U.S., Ye, Z., Martini, A., Tysoe, W.T.: Shear-induced mechanochemistry: pushing molecules around. J. Phys. Chem. C 119, 7115–7123 (2015)
- Rana, R., Bavisotto, R., Hopper, N., Tysoe, W.T.: Inducing highenergy-barrier tribochemical reaction pathways; acetic acid decomposition on copper. Tribol. Lett. 69, 32 (2021)
- Rana, R., Bavisotto, R., Hou, K., Tysoe, W.T.: Surface chemistry at the solid-solid interface: mechanically induced reaction pathways of C<sub>8</sub> carboxylic acid monolayers on copper. Phys. Chem. Chem. Phys. 23, 17803–17812 (2021)
- Rana, R., Bavisotto, R., Hou, K., Hopper, N., Tysoe, W.T.: Influence of the nature and orientation of the terminal group on the tribochemical reaction rates of carboxylic acid monolayers on copper. Tribol. Lett. 70, 5 (2021)
- Rana, R., Hopper, N., Sidoroff, F., Tysoe, W.T.: Critical stresses in mechanochemical reactions. Chem. Sci. 13, 12651–12658 (2022)
- 35. Furlong, O.J., Miller, B.P., Tysoe, W.T.: Shear-induced surface-to-bulk transport at room temperature in a sliding metal-metal interface. Tribol. Lett. **41**, 257–261 (2011)
- Bavisotto, R., Rana, R., Hopper, N., Hou, K., Tysoe, W.T.: Influence of the terminal group on the thermal decomposition reactions of carboxylic acids on copper: nature of the carbonaceous film. Phys. Chem. Chem. Phys. 23, 17663–17671 (2021)
- Rana, R., Djuidje Kenmoe, G., Sidoroff, F., Bavisotto, R., Hopper, N., Tysoe, W.T.: Anisotropy of shear-induced mechanochemical reaction rates of surface adsorbates; implications for theoretical models. J. Phys. Chem. C 126, 11585–11593 (2022)
- Jenks, C.J., Chiang, C.M., Bent, B.E.: Alkyl iodide decomposition on copper surfaces: alpha-elimination and beta-hydride

- elimination from adsorbed alkyls. J. Am. Chem. Soc. **113**, 6308–6309 (1991)
- Lin, J.L., Bent, B.E.: Carbon-halogen bond dissociation on copper surfaces: effect of alkyl chain length. J. Phys. Chem. 96, 8529– 8538 (1992)
- Jenks, C.J., Bent, B.E., Zaera, F.: The chemistry of alkyl iodides on copper surfaces 2 influence of surface structure on reactivity. J. Phys. Chem. B 104, 3017–3027 (2000)
- Gnecco, E., Roth, R., Baratoff, A.: Analytical expressions for the kinetic friction in the Prandtl–Tomlinson model. Phys. Rev. B 86, 035443 (2012)
- 42. Kauzmann, W., Eyring, H.: The viscous flow of large molecules. J. Am. Chem. Soc. **62**, 3113–3125 (1940)
- Gao, F., Furlong, O., Kotvis, P.V., Tysoe, W.T.: Pressure dependence of shear strengths of thin films on metal surfaces measured in ultrahigh vacuum. Tribol. Lett. 31, 99–106 (2008)
- Bavisotto, R., Rana, R., Hopper, N., Olson, D., Tysoe, W.T.: Adsorption and reaction pathways of 7-octenoic acid on copper. Phys. Chem. Chem. Phys. 23, 5834–5844 (2021)
- Bavisotto, R., Rana, R., Hopper, N., Hou, K., Tysoe, W.T.: Influence of the terminal group on the thermal decomposition reactions of carboxylic acids on copper. Phys. Chem. Chem. Phys. 23, 17663–17671 (2021)
- Bavisotto, R., Rana, R., Hopper, N., Tysoe, W.T.: Structure and reaction pathways of octanoic acid on copper. Surf. Sci. 711, 121875 (2021)
- Yan, J., Lien, H.-M., Mangolini, F.: Linking molecular structure and lubrication mechanisms in tetraalkylammonium orthoborate ionic liquids. Tribol. Lett. 71, 41 (2023)
- Gnecco, E., Bennewitz, R., Gyalog, T., Loppacher, C., Bammerlin, M., Meyer, E., et al.: Velocity dependence of atomic friction. Phys. Rev. Lett. 84, 1172–1175 (2000)
- Fusco, C., Fasolino, A.: Velocity dependence of atomic-scale friction: a comparative study of the one- and two-dimensional Tomlinson model. Phys. Rev. B 71, 045413 (2005)
- Müser, M.: Velocity dependence of kinetic friction in the Prandtl– Tomlinson model. Phys. Rev. B 84, 125419 (2011)
- Dorgham, A., Parsaeian, P., Azam, A., Wang, C., Morina, A., Neville, A.: Single-asperity study of the reaction kinetics of P-based triboreactive films. Tribol. Int. 133, 288–296 (2019)

**Publisher's Note** Springer Nature remains neutral with regard to jurisdictional claims in published maps and institutional affiliations.

Springer Nature or its licensor (e.g. a society or other partner) holds exclusive rights to this article under a publishing agreement with the author(s) or other rightsholder(s); author self-archiving of the accepted manuscript version of this article is solely governed by the terms of such publishing agreement and applicable law.

## **Authors and Affiliations**

Octavio J. Furlong<sup>1</sup> · Sergio J. Manzi<sup>1</sup> · Kaiming Hou<sup>2</sup> · Resham Rana<sup>3</sup> · Heather Adams<sup>3</sup> · Wilfred T. Tysoe<sup>3</sup>

- Wilfred T. Tysoe wtt@uwm.edu
- Instituto de Física Aplicada (INFAP), CONICET-Universidad Nacional de San Luis, Chacabuco 917, 5700 San Luis, Argentina
- State Key Laboratory of Solid Lubrication, Lanzhou Institute of Chemical Physics, Chinese Academy of Sciences, Lanzhou 730000, China
- Department of Chemistry and Biochemistry, and Laboratory for Surface Studies, University of Wisconsin-Milwaukee, Milwaukee, WI 53211, USA

